Carcinogen–Nucleic Acid Interactions: Equilibrium Binding Studies of Aflatoxin B_1 with the Oligodeoxynucleotide $d(ATGCAT)_2$ and with Plasmid pBR322 Support Intercalative Association with the B-DNA Helix†

S. Gopalakrishnan, Suzanne Byrd, Michael P. Stone,* and Thomas M. Harris
Department of Chemistry and Center in Molecular Toxicology, Vanderbilt University, Nashville, Tennessee 37235
Received June 1, 1988; Revised Manuscript Received August 22, 1988

ABSTRACT: Equilibrium binding of aflatoxin B_1 (AFB1) to the oligodeoxynucleotide $d(ATGCAT)_2$ was examined by using ^1H NMR. AFB1 binds to double-stranded $d(ATGCAT)_2$ with an apparent binding constant of 3.7×10^3 M^{-1}. The equilibrium is rapid on the NMR time scale; the observed ^1H NMR spectrum represents the population-weighted average of the chemical shifts arising from the free and bound states of the oligodeoxynucleotide and the AFB1. The spectrum of $d(ATGCAT)_2$ exhibits exchange broadening in the presence of AFB1, manifested as decreases in apparent T_2 relaxation times for the $d(ATGCAT)_2$ base protons. Upon binding to $d(ATGCAT)_2$, the AFB1 signals are shifted upfield, indicative of increased shielding. The adenine H2 protons are also shifted upfield in the presence of the carcinogen. Small changes in chemical shift are observed for other $d(ATGCAT)_2$ protons. A substantial decrease in the nonselective T_1 relaxation time is observed for the adenine H2 protons in the presence of AFB1. Competition binding experiments in which the competing ligands actinomycin D, ethidium bromide, and spermidine were individually added to an AFB1–$d(ATGCAT)_2$ equilibrium mixture showed that addition of 1 equiv of actinomycin D or 4 equiv of ethidium bromide was sufficient to displace bound AFB1 from $d(ATGCAT)_2$. In contrast, the addition of spermidine did not result in the displacement of bound AFB1 molecules and may have slightly enhanced binding, presumably due to stabilization of the DNA duplex. ^1H NOESY experiments confirmed that the overall conformation for the $d(ATGCAT)_2$ duplex was right-handed both in the absence and in the presence of AFB1. Equilibrium binding of AFB1 to $d(ATGCAT)_2$ is greatly diminished at higher temperatures at which the oligodeoxynucleotide is single-stranded. A series of experiments were performed in which the T_m of $d(ATGCAT)_2$ was increased by increasing the total oligodeoxynucleotide concentration; these experiments showed that AFB1 would bind to $d(ATGCAT)_2$ at higher temperatures provided that the DNA was in double-stranded form. Measurement of the overall binding equilibrium over the range 0–12 °C indicated that ΔH for the equilibrium binding of AFB1 to $d(ATGCAT)_2$ is ~ -1.2 kcal/mol. Binding of the mycotoxin to (a) negatively supercoiled and (b) relaxed closed circular plasmid pBR322 DNA was examined by using gel electrophoresis. Titration of negatively supercoiled plasmid with increasing amounts of AFB1 in tubular agarose gels showed a decrease in electrophoretic mobility due to unwinding of the plasmid. A similar titration of relaxed closed circular pBR322 DNA resulted in rewinding of the plasmid with introduction of positive supercoils. The critical free concentration of AFB1 was reached when approximately 50 μg/mL was added to the gels. The results of these experiments provide strong evidence that noncovalent binding of AFB1 to B-form DNA involves the intercalation of the mycotoxin between base pairs; this intercalation could direct subsequent covalent attachment of the carcinogen at the N7 position of guanine.

Aflatoxin B_1 is among the most potent of environmental mutagens and is implicated as a liver carcinogen; it is of world concern because of its widespread occurrence in corn, peanuts, cottonseed, and other food commodities. It is the most toxic among a family of highly toxic compounds containing the coumarin ring structure produced by *Aspergillus flavus* and *Aspergillus parasiticus*. The structure of AFB1[1] is shown in Figure 1, along with structures of three additional DNA binding ligands utilized in this work: ethidium bromide, actinomycin D, and spermidine. The covalent attachment of AFB1 to DNA in vivo is believed to occur via activation of the carcinogen by mixed-function oxidases. The ultimate carcinogen, aflatoxin B_1 8,9-epoxide, attacks the N7 position of guanine with high specificity and stereoselectivity [reviewed by Essigmann et al. (1983)]. Additional investigations (Muench et al., 1983; Misra et al., 1983; Marien et al., 1987; Benasutti et al., 1988) showed that specific guanine residues in double-stranded DNA appear to be high-affinity sites which show preferential covalent binding.

The selectivity for covalent attack at the N7 position of guanine and the high stereospecificity of binding at this

† This research was supported by funding from the National Institutes of Health (ES-00267 and ES-03755). S.B. acknowledges support from a training grant in molecular toxicology (ES-07028).

[1] Abbreviations: AFB1, aflatoxin B_1; AFB2, aflatoxin B_2; C_f, molar concentration of free AFB1; CPMG, Carr-Purcell-Meiboom-Gill pulse sequence; DMSO, dimethyl sulfoxide; DNA, deoxyribonucleic acid; DSS, sodium 4,4-dimethyl-4-silapentanesulfonate; EDTA, ethylenediaminetetraacetic acid; NMR, nuclear magnetic resonance; NOE, nuclear Overhauser effect; NOESY, two-dimensional nuclear Overhauser spectroscopy; r, $[AFB1]_{bound}/[d(ATGCAT)_2]$; T_m, melting temperature; T_1, spin–lattice relaxation; T_2, spin–spin relaxation; TAE, 2-amino-2-(hydroxymethyl)-1,3-propanediol/acetate/ethylenediaminetetraacetic acid buffer; TOPO, 2-amino-2-(hydroxymethyl)-1,3-propanediol/magnesium chloride/dithiothreitol/ethylenediaminetetraacetic acid buffer; TPPI, time-proportional phase increment; Tris, 2-amino-2-(hydroxymethyl)-1,3-propanediol; UV, ultraviolet; vis, visible; 2D, two-dimensional. The oligodeoxynucleotides discussed in this work do not have terminal phosphates, and the notation is abbreviated by leaving out the phosphodiester linkage.

0006-2960/89/0428-0726$01.50/0 © 1989 American Chemical Society

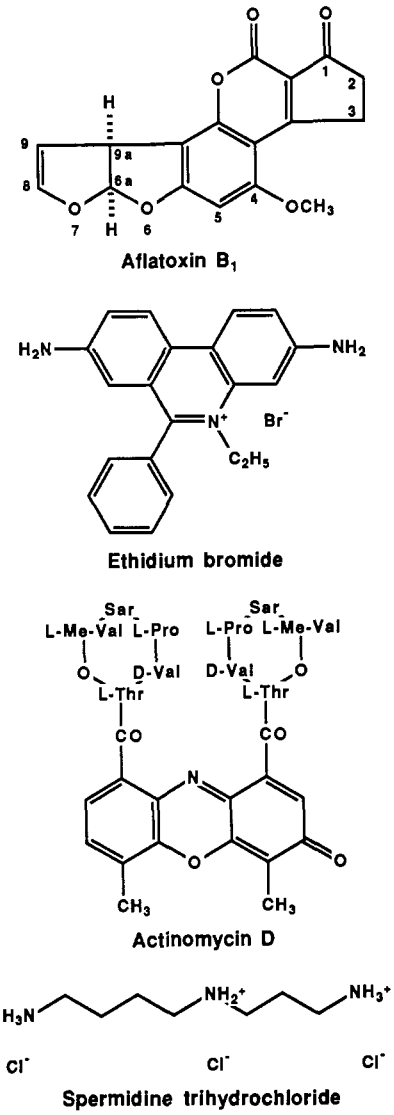

FIGURE 1: Chemical structures of aflatoxin B_1, ethidium bromide, actinomycin D, and spermidine. The numbering system is shown for the AFB1 molecule. The primary mode of interaction of the planar aromatic dye ethidium bromide with DNA is intercalation. Actinomycin D forms a complex with $d(ATGCAT)_2$ in which the planar phenoxazone chromophore intercalates at the GpC site and the two cyclic pentapeptide chains lie in the minor groove of the oligodeoxynucleotide. Spermidine forms a tight complex with the oligodeoxynucleotide, presumably resulting from groove binding.

position suggests that the covalent reaction may be mediated by precovalent equilibrium binding, the orientation of which controls the stereochemistry of covalent attachment (Misra et al., 1983; Loechler et al., 1988). In this report, we present results from ^1H NMR spectroscopic studies of the noncovalent interactions of AFB1 with the oligodeoxynucleotide $d(ATGCAT)_2$. These results are supportive of an intercalation model for the precovalent interaction of the carcinogen with this oligodeoxynucleotide. In addition, we present corroborating evidence for precovalent intercalation of the carcinogen, as derived from gel electrophoresis experiments of the interaction of the carcinogen with the DNA plasmid pBR322.

Materials and Methods

Materials. AFB1 (Sigma), ethidium bromide (Sigma), topoisomerase I (Promega), the plasmid pBR322 (BRL), and all oligodeoxynucleotide synthesis reagents (Pharmacia/P-L Biochemicals) were purchased. *Crystalline AFB1 is extremely hazardous due to its electrostatic nature and should be handled using containment procedures and respiratory mask to prevent inhalation.* d(ATGCAT) was synthesized by using standard solid-phase phosphoramidite chemistry with an automated synthesizer. The amount of single-stranded hexadeoxynucleotide was measured by using an extinction coefficient of 42,500 M^{-1} cm^{-1} at 260 nm.

Nuclear Magnetic Resonance. ^1H NMR frequencies of 300.13 or 400.13 MHz were utilized. For preparation of oligodeoxynucleotide NMR samples in D_2O, 400 μL of NMR buffer (0.1 M NaCl, 5×10^{-5} M Na_2EDTA, and 0.01 M sodium phosphate, pH 7.0) was added to the desired amount of $d(ATGCAT)_2$. Samples were lyophilized three times from D_2O and then dissolved in 400 μL of 99.96% D_2O. AFB1 is sparingly soluble in aqueous solution; solubility is a limitation in the examination of equilibrium systems using NMR. Inclusion of DMSO in the aqueous solution increased the solubility of AFB1. The concentration of a saturated AFB1 solution in NMR buffer in the absence of DMSO was determined to be 0.03 mM and increased to 0.09 mM with the inclusion of 2.5% DMSO. Therefore, 2.5% DMSO-d_6 was added to samples prepared for NMR measurements. Some NMR experiments in the presence of $d(ATGCAT)_2$ were performed under conditions in which the total amount of AFB1 present in solution exceeded the aqueous solubility of free AFB1. In other experiments a saturated solution was in equilibrium with crystalline AFB1; under these conditions the amount of unbound AFB1 remained constant and independent of the amount of oligodeoxynucleotide present. 2D NOE (NOESY) experiments were performed by using a sample that contained a saturated AFB1 solution in equilibrium with 13.5 mM $d(ATGCAT)_2$. These experiments were performed by using the TPPI (Bodenhausen et al., 1984) phase-sensitive pulse sequence, with gated decoupling to suppress the residual HDO signal. T_1 experiments were performed by using the standard inversion–recovery pulse sequence, and T_2 experiments utilized the CPMG spin-echo method. Chemical shifts were referenced internally to DSS; sample temperature was controlled to within 0.5 °C.

Equilibrium Binding Experiments. A 0.074 mM sample of AFB1 in D_2O (NMR buffer, as above) was titrated with $d(ATGCAT)_2$ dissolved in deuteriated NMR buffer containing 0.074 mM AFB1. This concentration was below the saturation limit for the carcinogen. Thus, the total concentration of AFB1 in solution remained constant, but the fraction bound varied as a function of the amount of oligodeoxynucleotide added to the system. The chemical shifts of the various AFB1 protons were plotted as a function of equivalents of $d(ATGCAT)_2$ added to the solution. Limiting chemical shifts for various AFB1 protons in the bound state were estimated by extrapolation to infinite $d(ATGCAT)_2$ concentration.

Competitive Binding Experiments. Ethidium bromide and actinomycin D were dissolved in D_2O and quantitated by using extinction coefficients of 5860 M^{-1} cm^{-1} (480 nm) and 24 400 M^{-1} cm^{-1} (440 nm), respectively. Spermidine trihydrochloride was prepared by weight and diluted to a stock concentration of 10 mM in D_2O. NMR samples for competitive binding experiments were 0.5 mM in $d(ATGCAT)_2$ and contained a saturated solution of AFB1 (in the presence of 2.5% DMSO-d_6). A parallel experiment was performed on a saturated sample of AFB1 with no oligodeoxynucleotide present. As the competing ligand was titrated into the two samples, the AFB1 chemical shifts in the sample containing the oligodeoxynucleotide were compared to those in the parallel sample containing no oligodeoxynucleotide. The blank sample served to control any contribution in the observed chemical shift of

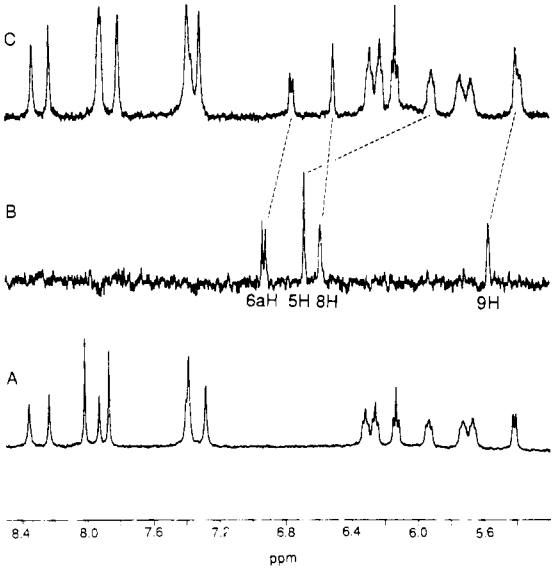

FIGURE 2: A comparison of the 1D ^{1}H NMR spectrum at 5 °C of (A) d(ATGCAT)$_2$, (B) AFB1, and (C) the equilibrium mixture of AFB1 and d(ATGCAT)$_2$. The dotted lines show the change in chemical shift for selected AFB1 protons in the presence of the oligodeoxynucleotide. The three spectra were processed in the same manner but contain differing numbers of acquisitions, resulting in the difference in S/N. Increased line width due to exchange broadening is visible in the spectrum of the equilibrium mixture.

the carcinogen derived from interaction of the AFB1 with the competing ligand.

Electrophoresis Experiments. Closed circular plasmid pBR322 was subjected to electrophoresis on a series of cylindrical agarose gels which contained increasing amounts of AFB1 according to the procedure of Espejo and Lebowitz (1976). A 1% (w/v) solution of agarose was prepared by dissolving agarose in TAE buffer (40 mM Tris, 5 mM sodium acetate, and 1 mM Na_2EDTA, pH 8.0). AFB1 was dissolved in DMSO to form a concentrated stock solution, and differing aliquots of this stock solution were added to the series of gels. The amounts added ranged from 0 to 55 μg/mL. The loading buffer for the pBR322 consisted of TAE, with the addition of 10% sucrose and 0.04% bromphenol blue. A 10-μL aliquot (0.27 μg) of the plasmid in loading buffer was layered on each tube gel and subjected to electrophoresis at 60 V for 4–6 h. The gels were stained with a solution of ethidium bromide (0.5 μg/mL) and then visualized by short-wave UV light and photographed. For the samples that were treated with topoisomerase I, 4 μL of 10 × TOPO buffer (0.5 M Tris-HCl, 0.5 M KCl, 0.1 M $MgCl_2$, 5 mM dithiothreitol, and 1 mM Na_2EDTA, pH 7.5), 1–10 μg of pBR322, and 10 units (1 μL) of topoisomerase I were combined with water to a volume of 40 μL and incubated at 37 °C for 5 h. The enzyme-treated DNA was then diluted with loading buffer to a concentration equivalent to the untreated plasmid (0.27 μg of DNA in 10 μL of loading buffer) and subjected to electrophoresis at 60 V for 4–6 h.

Results

NMR Spectra of an Equilibrium Mixture of AFB1 and 0.5 mM d(ATGCAT)$_2$. Figure 2 shows the 400-MHz ^{1}H NMR spectra of d(ATGCAT)$_2$, AFB1, and a mixture in which 0.5 mM d(ATGCAT)$_2$ is in equilibrium with a saturated solution of AFB1, obtained at 5 °C. The concentration of free AFB1 in the saturated solution was measured to be 0.09 mM. Integration of the AFB1 signals in the equilibrium mixture revealed the total amount in solution to be 0.25 mM. The fraction bound to the oligodeoxynucleotide under these conditions is 0.64 (0.16 mM). The AFB1–oligodeoxynucleotide complex is in rapid exchange under the conditions studied; the resulting NMR spectrum (Figure 2C) consists of an average spectrum in which the observed chemical shifts represent the population-weighted averages of the various species in rapid exchange. These species consist of unbound AFB1, free oligodeoxynucleotide, and all species in which one or more AFB1 molecules are bound to d(ATGCAT)$_2$. The observed chemical shift changes for selected oligodeoxynucleotide and AFB1 protons for this sample are given in Tables I and II. Since the oligodeoxynucleotide is in excess, the observed chemical shift changes for the d(ATGCAT)$_2$ protons are small, the largest changes being observed for the two adenine H2 protons (0.06 and 0.09 ppm upfield shifts, respectively). In contrast, a significant increase in shielding is observed for the AFB1 protons under these conditions, ranging in magnitude from the 0.08 ppm upfield shift of the 8H proton to 0.72 ppm for the 5H proton. Increasing the amount of d(ATGCAT)$_2$ in solution increases the fraction of bound AFB1 and results in larger chemical shift changes for the AFB1 protons.

Table I: Chemical Shift Changes Observed for Selected d(ATGCAT)$_2$ Protons in an Equilibrium Mixture of d(ATGCAT)$_2$ and AFB1 at 5 °C[a]

proton	chemical shift (ppm), d(ATGCAT)$_2$–AFB1	chemical shift (ppm), d(ATGCAT)$_2$	Δδ
AH8 (internal)	8.33	8.35	−0.02
AH8 (terminal)	8.23	8.23	0.00
AH2 (terminal)	7.92	8.01	−0.09
GH8	7.91	7.93	−0.02
AH2 (internal)	7.81	7.87	−0.06
TH6 (internal)	7.39	7.38	0.01
TH6 (terminal)	7.32	7.28	0.04
CH5	5.40	5.41	−0.01
T-CH_3 (terminal)	1.53	1.52	0.01
T-CH_3 (internal)	1.38	1.38	0.00
AH1′ (internal)	6.29	6.32	−0.03
AH1′ (terminal)	6.23	6.26	−0.03
TH1′ (terminal)	6.13	6.13	0.00
GH1′	5.92	5.93	−0.01
TH1′ (internal)	5.74	5.73	0.01
CH1′	5.68	5.67	0.01

[a] The concentration of free AFB1 in the solution was measured to be 0.09 mM, and the total amount of AFB1 in solution was measured to be 0.25 mM. The concentration of d(ATGCAT)$_2$ was 0.5 mM (3 mM base pairs).

Table II: Chemical Shift Changes Observed for Selected AFB1 Protons in an Equilibrium Mixture of d(ATGCAT)$_2$ and AFB1 at 5 °C[a]

proton	chemical shift (ppm), AFB1	chemical shift (ppm), d(ATGCAT)$_2$–AFB1	Δδ
6a	6.93	6.76	−0.17
5	6.69	5.97	−0.72
8	6.59	6.51	−0.08
9	5.57	5.40	−0.17
4-OCH_3	3.98	3.72	−0.26

[a] The concentration of free AFB1 in the solution was measured to be 0.09 mM, and the total amount of AFB1 in solution was measured to be 0.25 mM. The concentration of d(ATGCAT)$_2$ was 0.5 mM (3 mM Base pairs).

Equilibrium of the AFB1–d(ATGCAT)$_2$ Complex. The AFB1–d(ATGCAT)$_2$ equilibrium was examined by the titration of a 0.074 mM solution of AFB1 with d(ATGCAT)$_2$ at 5 °C. These data are shown in Figure 3, from which it may be concluded that, even at a 25-fold molar excess of d(ATGCAT)$_2$, the observed chemical shifts of the AFB1

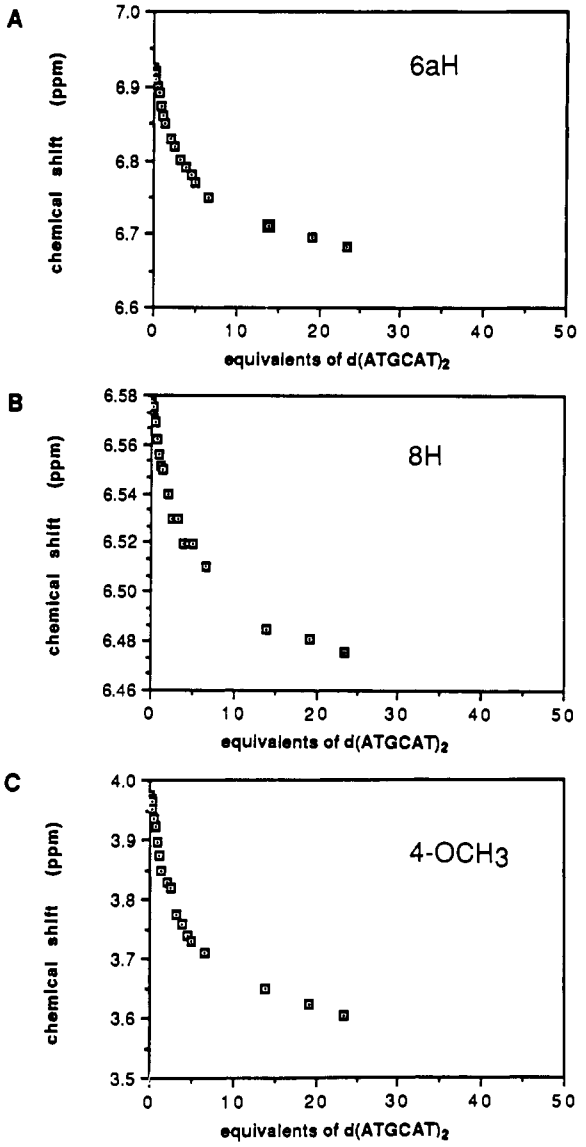

FIGURE 3: Titration of a 0.074 mM solution of AFB1 with $d(ATGCAT)_2$. (A–C) The chemical shifts of selected AFB1 protons are shown as a function of equivalents of $d(ATGCAT)_2$ added. The limiting chemical shifts for the AFB1 6aH, 8H, and 4-OCH_3 protons in the bound state were estimated by extrapolation of the data to be 6.65, 6.46, and 3.54 ppm, respectively.

protons have not reached limiting values characteristic of the bound state. These limiting chemical shifts were estimated from extrapolation of the data shown in Figure 3 to infinite oligodeoxynucleotide concentration. The concentration of bound AFB1 was calculated from the estimated limiting chemical shifts of the carcinogen and the total amount of carcinogen in solution. The fraction of free and bound carcinogen was evaluated as a function of the amount of oligodeoxynucleotide present in the system. The binding data are displayed as a Scatchard plot in Figure 4.

Temperature Dependence of the Equilibrium between AFB1 and d(ATGCAT)$_2$. Figure 5 presents the results for an experiment in which the chemical shifts of various AFB1 protons in the AFB1–$d(ATGCAT)_2$ equilibrium mixture are plotted as a function of temperature. The experiment was repeated at four concentrations of $d(ATGCAT)_2$: 0.5, 2.0, 4.0, and 13.5 mM. Inspection of Figure 5A, a δ vs temperature plot of the $d(ATGCAT)_2$ cytosine H5 proton at the four different concentrations, shows the T_m of $d(ATGCAT)_2$ is shifted to higher temperature as oligodeoxynucleotide concentration is increased, consistent with expectation. Comparison of Figure 5B with

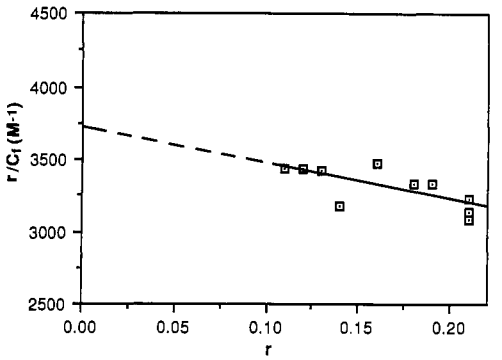

FIGURE 4: Scatchard plot of the titration data shown in Figure 3. Analysis of the Scatchard data gives a value for the intrinsic association constant $K = 3.7 \times 10^3$. The line drawn through the data represents the least-squares fit of the data. $r = [AFB1]_{bound}/[d(ATGCAT)_2]$; $C_f = [AFB1]_{free}$.

Table III: Observed Changes in T_2 for Selected $d(ATGCAT)_2$ Protons in the Absence and in the Presence of AFB1, As Measured by Using the CPMG Spin-Echo Technique at 5 °C[a]

proton	T_2 (s), $d(ATGCAT)_2$–AFB1	T_2 (s), $d(ATGCAT)_2$	ΔT_2 (s)
AH8 (internal)	0.066	0.073	−0.007
AH8 (terminal)	0.11	0.12	−0.010
AH2 (terminal)	0.18[b]	0.24	−0.060[b]
GH8	0.075[b]	0.15	−0.075[b]
AH2 (internal)	0.23	0.34	−0.11
TH6 (terminal)	0.081	0.12	−0.039
T-CH_3 (internal)	0.076	0.10	−0.024
T-CH_3 (terminal)	0.076	0.10	−0.024

[a] The concentration of $d(ATGCAT)_2$ was 1.0 mM (6 mM base pairs). The GH8 and AH2 (terminal) protons overlap in the spectrum, making intensity measurements uncertain. [b] Estimated changes due to spectral overlap in the equilibrium mixture of AFB1 and $d(ATGCAT)_2$.

Figure 5A shows that the midpoint of the curve representing the cooperative dissociation of AFB1 from $d(ATGCAT)_2$ is also shifted to higher temperature as $d(ATGCAT)_2$ concentration is increased.

The value of ΔH for the binding of AFB1 to $d(ATGCAT)_2$ was estimated from a 4 mM solution of $d(ATGCAT)_2$ in the presence of saturated AFB1; under these conditions only the highest affinity binding sites are likely to be filled. The apparent macroscopic binding constant, $K_{apparent}$, was measured as a function of temperature in the region of the melting curve below T_m (0–12 °C). A graph of ln $K_{apparent}$ vs $1/T$ for this temperature range is shown in Figure 6. The results of this experiment indicate that the position of the equilibrium changes only slightly over this temperature range; ΔH is estimated to be −1.2 kcal/mol.

NMR Line Shapes of Selected d(ATGCAT)$_2$ Protons upon Addition of AFB1 to the Sample. The chemical shifts of various $d(ATGCAT)_2$ protons differ in the bound and free state; these chemical shift changes are evidenced by exchange broadening of oligodeoxynucleotide signals in the presence of AFB1. Visual inspection of the spectra indicates that the aromatic resonances of $d(ATGCAT)_2$ are broadened in the presence of the carcinogen molecule. This exchange broadening of the resonances was examined by measurement of apparent spin–spin relaxation times using the CPMG spin-echo method. As compared to observed T_2 relaxation times for $d(ATGCAT)_2$, apparent spin–spin relaxation times measured for $d(ATGCAT)_2$ in the presence of AFB1 give a measure of the effect of exchange broadening at particular sites on the oligodeoxynucleotide molecule (Table III). A decrease in T_2 is observed for $d(ATGCAT)_2$ aromatic and thymine CH_3

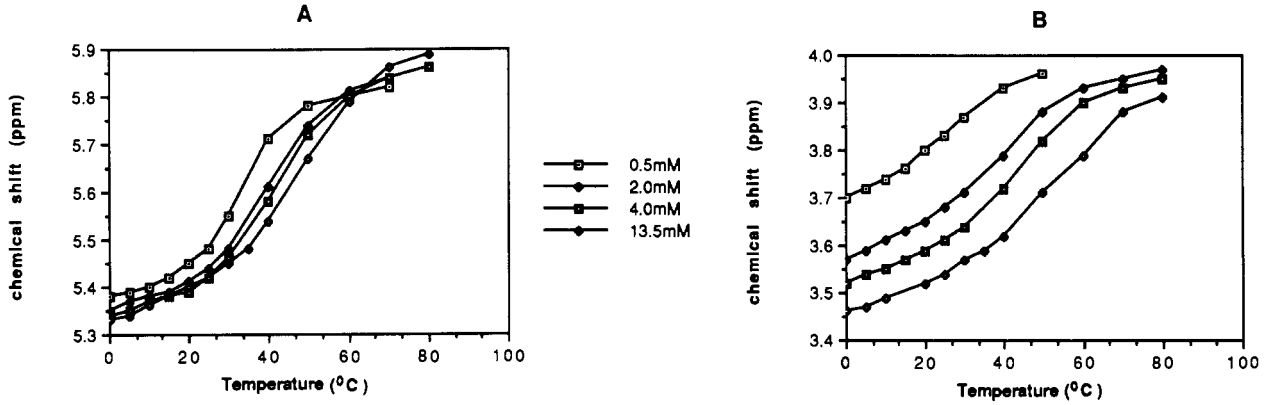

FIGURE 5: (A) Chemical shift of the d(ATGCAT) cytosine H5 proton as a function of temperature at four oligodeoxynucleotide concentrations. As the temperature of the sample is increased, $d(ATGCAT)_2$ undergoes the melting transition to the single-stranded random coil. The midpoint of this transition (T_m) increases at higher concentration. (B) Chemical shift of the AFB1 4-OCH_3 protons as a function of temperature. At higher temperatures where the oligodeoxynucleotide is single-stranded, AFB1 dissociates from the oligodeoxynucleotide. At higher oligodeoxynucleotide concentration the dissociation of AFB1 from the oligodeoxynucleotide is shifted to higher temperature.

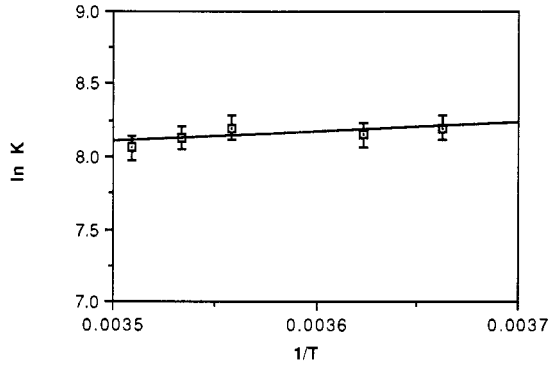

FIGURE 6: The logarithm of the apparent binding constant plotted as a function of inverse temperature (K) over the range 0–12 °C, below the melting transition of the oligodeoxynucleotide. The concentration of $d(ATGCAT)_2$ was 4 mM. Analysis of the van't Hoff plot indicates that, over this range of temperature, ΔH for the binding of AFB1 to $d(ATGCAT)_2$ is ~ -1.2 kcal/mol. Error bars represent the range of the 80% confidence level in the measurements of K.

Table IV: Nonselective T_1 Relaxation Rate Changes Observed for Selected $d(ATGCAT)_2$ Protons in an Equilibrium Mixture of $d(ATGCAT)_2$ and AFB1 at 5 °C[a]

proton	T_1 (s), $d(ATGCAT)_2$–AFB1	T_1 (s), $d(ATGCAT)_2$	ΔT_1 (s)
AH8 (internal)	1.0	1.2	−0.2
AH8 (terminal)	1.5	1.5	0.0
AH2 (terminal)	3.7	4.3	−0.6
GH8	1.4	1.5	−0.1
AH2 (internal)	3.7	4.2	−0.5
TH6 (terminal)	1.2	1.4	−0.2

[a] The concentration of free AFB1 in the solution was measured to be 0.09 mM, and the total amount of AFB1 in solution was measured to be 0.25 mM. The concentration of $d(ATGCAT)_2$ was 0.5 mM (3 mM base pairs).

protons in the presence of AFB1. The greatest changes are observed for the aromatic protons of the A·T base pairs, including the two AH2 protons, the terminal TH6 proton, and the two sets of T CH_3 protons.

Nonselective Spin–Lattice Relaxation Measurements on the AFB1–d(ATGCAT)$_2$ Equilibrium Complex. Table IV contains the nonselective spin–lattice relaxation times observed for various protons of a 0.5 mM sample of $d(ATGCAT)_2$ in the absence and in the presence of 0.25 mM AFB1. Significant decreases of the relaxation time are observed for the adenine H2 protons in the presence of AFB1: the observed value of T_1 for the AH2 (terminal) proton decreases from 4.3 to 3.7 s (14%), and the observed value for the AH2 (internal) proton decreases from 4.2 to 3.7 s (12%). These results are similar to previous results obtained for the interaction of aflatoxin B_2 with this sequence (Stone et al., 1988).

Competitive Binding Experiments. Figure 7A illustrates the changes in the observed chemical shifts of various AFB1 protons as the equilibrium between the carcinogen and $d(ATGCAT)_2$ is altered by the addition of ethidium bromide. The observed chemical shifts of the AFB1 protons are plotted as a function of the ratio [ethidium bromide]:[$d(ATGCAT)_2$].

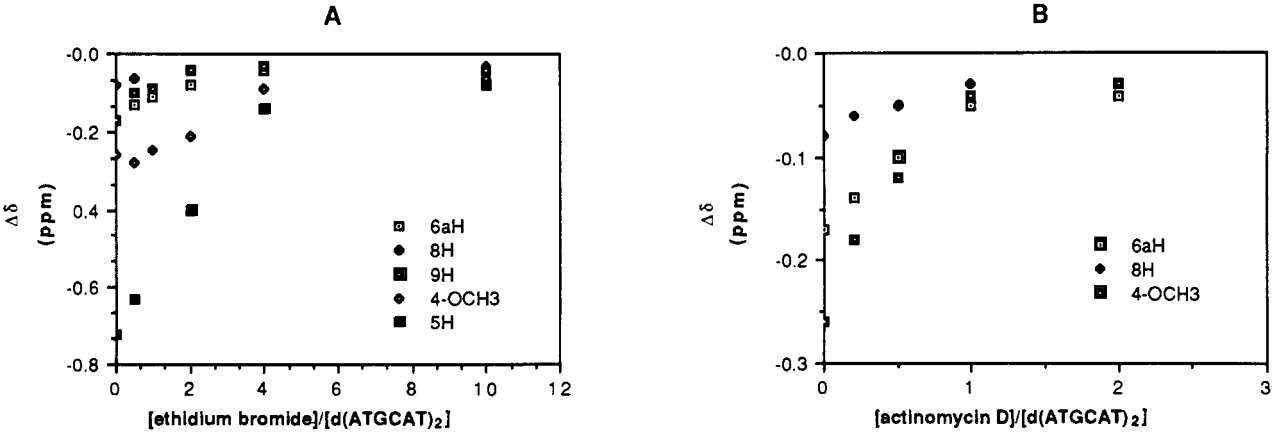

FIGURE 7: Chemical shift of the various AFB1 proton resonances as a function of (A) [ethidium bromide]/[$d(ATGCAT)_2$] and (B) [actinomycin D]/[$d(ATGCAT)_2$]. As the competing ligand is titrated into the equilibrium mixture, AFB1 is displaced from $d(ATGCAT)_2$.

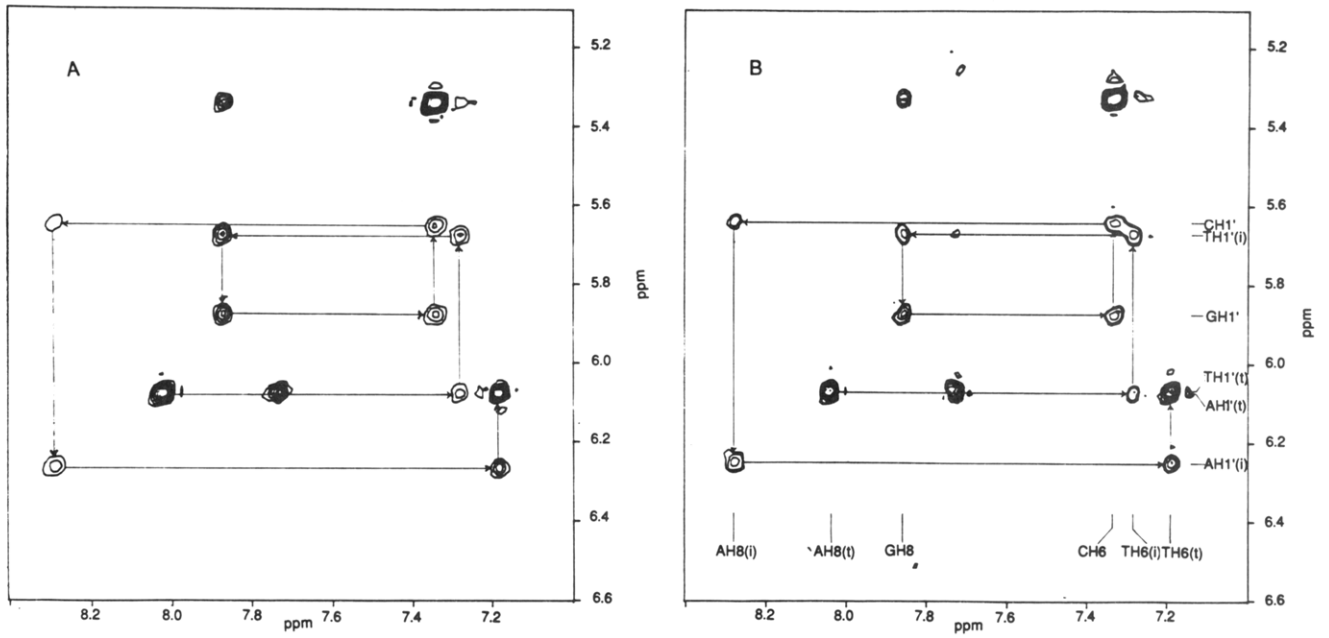

FIGURE 8: NOESY data for a 13.5 mM sample of $d(ATGCAT)_2$ in (A) NMR buffer and (B) NMR buffer containing AFB1. The cross-peaks shown represent the dipolar coupling interactions between the deoxyribose anomeric protons and the purine H8 or pyrimidine H6 protons.

The chemical shifts of the AFB1 protons approach the chemical shifts of free AFB1 as the [ethidium]:[duplex] ratio reaches 4.0, indicating that, at a ratio of 4 ethidiums per duplex, the AFB1 molecules are displaced from the DNA. This experiment was repeated with actinomycin D; the results are shown in Figure 7B. When the molar ratio of [actinomycin D] to $[d(ATGCAT)_2]$ is 1:1, the AFB1 molecules are entirely displaced from the oligodeoxynucleotide. In contrast to the results observed for ethidium bromide and actinomycin D, when spermidine trihydrochloride was titrated into the AFB1–oligodeoxynucleotide equilibrium mixture, AFB1 was not displaced.

2D NOE Spectroscopy. Figure 8 shows a portion of the phase-sensitive (TPPI) NOESY contour plot for a 13.5 mM solution of $d(ATGCAT)_2$ in the absence and in the presence of AFB1. The pattern of NOE connectivities between the purine H8, pyrimidine H6, and deoxyribose H1′ protons indicates that the overall conformation of the oligodeoxynucleotide duplex is consistent with the B-DNA conformation [reviewed by Wüthrich (1986)]. In the presence of the AFB1, changes in the location of the cross-peaks are observed. The fraction of oligodeoxynucleotide in the bound state is low, and the chemical shift changes for the DNA cross-peaks are small.

Gel Electrophoresis. Figure 9 shows the results of AFB1 titrations of supercoiled and relaxed circular pBR322 DNA, monitored by gel electrophoresis. As seen in the first set of gels, increasing amounts of AFB1 cause an unwinding of the supercoiled plasmid. The amount of AFB1 that causes negatively supercoiled plasmid to comigrate with nicked circular DNA [the critical free concentration (c')] was reached when ~50 μg/mL AFB1 was added (lane j, Figure 9A). This is near the maximum solubility of AFB1 in TAE buffer (the molar concentration of AFB1 in each cylindrical gel was not measured). A second experiment was performed, in which the supercoiled pBR322 was relaxed by treatment with topoisomerase I and then electrophoresed in the presence of increasing amounts of AFB1 as before. Addition of carcinogen molecules into relaxed closed circular plasmid leads to the incorporation of positive supercoils, seen in Figure 9B as an increase in electrophoretic migration rate with increasing carcinogen concentration.

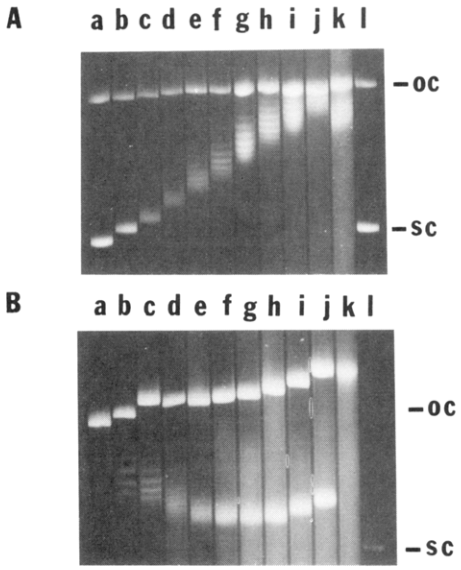

FIGURE 9: (A) Conformational changes in pBR322 caused by noncovalent interaction with AFB1. Electrophoretic titration of supercoiled pBR322 was performed in 1% agarose as described under Materials and Methods. The amount of AFB1 (μg/mL) added to each lane was as follows: lane a, 0.0 (control); lane b, 10.0; lane c, 15.0; lane d, 20.0; lane e, 25.0; lane f, 30.0; lane g, 35.0; lane h, 40.0; lane i, 45.0; lane j, 50.0; lane k, 55.0; lane l, 0.0 (control). The speckled appearance of lane k is due to partial precipitation of AFB1 at this concentration. OC = open circular; SC = supercoiled. (B) Electrophoretic titration of enzymatically relaxed pBR322 with AFB1 as described under Materials and Methods. The amount of AFB1 (μg/mL) added to each lane was as follows: lane a, 0.0 (control); lane b, 10.0; lane c, 15.0; lane d, 20.0; lane e, 25.0; lane f, 30.0; lane g, 35.0; lane h, 40.0; lane i, 45.0; lane j, 50.0; lane k, 55.0; lane l, 0.0 (control). Tubes a–j were loaded with enzymatically relaxed pBR322 while tubes *k* and l were loaded with native pBR322 to demonstrate the presence of supercoiled plasmid in the absence of AFB1 (l) and the loss of superhelicity with saturating amounts of AFB1 (k).

Discussion

Equilibrium between AFB1 and the Oligodeoxynucleotide $d(ATGCAT)_2$. AFB1 spontaneously forms noncovalent complexes with a variety of polymeric nucleic acids, and (at low temperature) with the oligodeoxynucleotide $d(ATGCAT)_2$.

Evidence for the formation of noncovalent complexes is derived from a number of different approaches, including UV–vis spectroscopy (Sporn et al., 1966; Clifford & Rees, 1967; King & Nicholson, 1969; Fujimoto & Ohba, 1975; Stone et al., 1988), equilibrium dialysis (Black & Jirgensons, 1967), and fluorescence spectroscopy (Neely et al., 1970).

Equilibrium binding of AFB1 to $d(ATGCAT)_2$ is potentially complex, as there are likely to be multiple binding sites on the oligodeoxynucleotide for the carcinogen. *Covalent* AFB1–DNA binding occurs at dG·dC base pairs to form guanine N7–AFB1 adducts (Essigmann et al., 1977, 1983). In contrast, UV–vis binding studies on a variety of polymeric DNAs and synthetic copolymers (Sporn et al., 1966; Clifford & Rees, 1967; King & Nicholson, 1969; Stone et al., 1988) show that noncovalent binding occurs at dA·dT as well as dG·dC base pairs. At high oligodeoxynucleotide:carcinogen ratios, binding sites having the highest affinity constants are expected to be occupied. In the case of multiple binding sites for the carcinogen, these binding sites could be characterized by different affinity and may not be independent. Analysis of noncovalent aflatoxin B_1 and B_2 binding to poly(dA-dT)·poly(dA-dT) and poly(dG-dC)·poly(dG-dC) indicated that the affinity constants for the two alternating sequences are comparable but not equivalent: poly(dA-dT)·poly(dA-dT) appears to have somewhat greater binding affinity for the carcinogen (Stone et al., 1988).

Weak binding data as are shown in Figure 3 are better characterized in the form of a Scatchard plot. Figure 4 shows that the Scatchard plot for binding of AFB1 to $d(ATGCAT)_2$ is linear over the range of r values that were examined. Extrapolation of the data to the y intercept yields an intrinsic association constant of $\sim 3.7 \times 10^3\ M^{-1}$. Extrapolation of the Scatchard data either to lesser or greater r values is speculative because of the small range of r values which are accessible in the experiment. However, it is interesting to note that UV measurements of AFB1 binding to calf thymus DNA, which included data obtained at lower r values, indicated that AFB1 binds with apparent positive cooperativity as is evidenced by concave-downward Scatchard plots derived from UV–vis binding isotherms (Stone et al., 1988).

Relationship between the Precovalent Orientation of AFB1 and the Subsequent Covalent Adduct That Is Formed. The relative extent of covalent modification of various guanine residues in double-stranded DNA depends on the nearest-neighbor sequence at specific guanines, and it appears that empirical rules to predict reactivity for specific guanines may be formulated (Misra et al., 1983; Marien et al., 1987; Benasutti et al., 1988). Misra et al. (1983) discussed two possible mechanisms mediating the sequence specificity of AFB1 covalent adduct formation. In the first model, the carcinogen diffuses freely along the lattice, but different G residues have differing reactivity. In the second model, the G residues have equal reactivity, but the carcinogen preferentially binds to particular high-affinity sites, followed by subsequent covalent attack. A major argument against the first model is the observed low reactivity of AFB1 toward single-stranded DNA; the free-diffusion model would presumably not require duplex DNA.

The utilization of $d(ATGCAT)_2$ to study the binding equilibrium allowed examination of the relationship between the single strand–double strand equilibrium and the binding affinity of AFB1. Our results indicate that equilibrium binding to $d(ATGCAT)_2$ exhibits a marked preference for the duplex state. The enthalpy for binding to $d(ATGCAT)_2$, although apparently negative, is relatively low (~ -1.2 kcal/mol). Under conditions in which this oligodeoxynucleotide is in the single-stranded state, binding of AFB1 is negligible, as can be determined from inspection of Figure 5. The melting transition of $d(ATGCAT)_2$ occurs cooperatively, evidenced by the sigmoidal plot that is obtained when the chemical shifts of the oligodeoxynucleotide are plotted as a function of temperature. The dissociation of AFB1 from $d(ATGCAT)_2$ as temperature is increased also results in a sigmoidal plot, indicative of a cooperative process. Figure 5 shows that as the T_m of the single strand–duplex equilibrium for $d(ATGCAT)_2$ is increased, the effective temperature midpoint for the dissociation of AFB1 from $d(ATGCAT)_2$ also increases. Our results are consistent with the second model described above, in which the carcinogen preferentially binds to particular high-affinity sites, and suggest that these sites are dependent upon maintenance of the B-DNA duplex.

The observed changes in chemical shift, line width, and T_1 of the adenine H2 protons as a function of addition of AFB1 are of particular interest because these protons in B-DNA are oriented such that they face into the minor groove, away from the covalent binding site at N7 of guanine, in the major groove. This suggests that a portion of the AFB1 molecule is in or adjacent to the minor groove of the DNA when the carcinogen is bound to the DNA. If the noncovalent AFB1 binding site were entirely contained within the minor groove, it could be concluded that noncovalent binding does not lead directly to formation of covalent AFB1 DNA adducts. T_2 changes are also observed for dA·dT base pair protons facing the major groove of the DNA, which suggests that the equilibrium binding site for the carcinogen is not exclusively within the minor groove of the oligodeoxynucleotide. The large upfield chemical shift changes observed for the AFB1 protons upon complexation with $d(ATGCAT)_2$ also do not appear consistent with a model where the carcinogen is contained within the minor groove of the oligodeoxynucleotide. Instead, we favor a model in which noncovalently bound AFB1 intercalates between base pairs and spans the oligodeoxynucleotide, resulting in changes for DNA protons in both the major and minor groove.

Evidence Supporting Intercalation as a Model for Precovalent Orientation of AFB1. Intercalation of AFB1 in the noncovalent AFB1–$d(ATGCAT)_2$ complex appears to be a reasonable hypothesis due to the planar nature of the coumarin chromophore. The intercalation model derives support from the observation that AFB1 is capable of forming photoadducts with DNA (Israel-Kalinsky et al., 1982; Misra et al., 1983); these photoadducts may result from 2 + 2 cycloadditions between DNA bases and the coumarin chromophore of AFB1, analogous to the well-characterized photoadducts formed between psoralen and DNA (Straub et al., 1981; Kanne et al., 1982), but their structures have not been investigated.

The observed chemical shift changes for the AFB1 protons upon interacting with $d(ATGCAT)_2$ are substantial (0.1–0.7 ppm increased shielding; Table II) and clearly consistent with the intercalation model for the interaction. In the intercalated state, the chemical shifts for AFB1 protons would be influenced by ring-current effects arising from interactions with the adjacent aromatic rings of the nucleotide bases. These ring-current shielding effects are expected to be as large as 1.5 ppm (Giessner-Prettre & Pullman, 1976, 1982; Giessner-Prettre et al., 1976, 1981). By varying the $d(ATGCAT)_2$ concentration to increase the fraction of AFB1 in the bound state, we have observed upfield chemical shifts up to ~ 1.4 ppm for the AFB1 5H proton.

The interaction of actinomycin D with DNA has been characterized by using both crystallographic (Sobell & Jain, 1972; Takusagawa et al., 1982) and NMR methods (Krugh & Neely, 1973; Patel, 1974; Krugh & Chen, 1975; Chiao & Krugh, 1977). The phenoxazone chromophore intercalates at the dG·dC base pair, while the cyclic peptide side chains of this drug form specific hydrogen-bonding interactions in the minor groove of B-DNA. The overall span of the actinomycin D molecule is about 4–5 base pairs in the double helix. The binding constant of actinomycin D to polymeric DNA is $\sim 10^6$ (Rosenberg et al., 1982).

The binding of ethidium bromide to DNA has also been well characterized by a variety of methods (LePecq, 1971; Reinhardt & Krugh, 1978; Winkle et al., 1981) and exhibits a binding constant ($\sim 10^5$) substantially greater than that for AFB1. NMR studies using dinucleotides showed a preference for pyrimidine(3′–5′)purine sequences (Krugh & Reinhardt, 1975), although the planar drug will intercalate between other sequences as well.

The polyamine spermidine forms a tight complex with B-DNA, evidenced by measurements of (a) the spermidine activity coefficient in the presence of DNA, (b) reduced electrophoretic mobility of DNA in the presence of spermidine, and (c) increase in the melting temperature of DNA in the presence of spermidine (Liquori et al., 1967). The particular stability of DNA–spermidine complexes is believed to result from the ability of spermidine to bind to B-DNA such that bridging hydrogen bonds between phosphate groups of the two DNA strands are formed (Liquori et al., 1967; Suwalsky et al., 1969; Woo et al., 1979; Drew & Dickerson, 1981). A binding site for the related molecule spermine in B-DNA in the solid state was defined when a crystal structure was solved for the dodecamer $d(CGCGAATTCGCG)_2$ grown in the presence of spermine (Drew & Dickerson, 1981). In this structure, spermine was found to straddle the major groove of the dodecamer and form bridging hydrogen bonds with the two oligodeoxynucleotide chains. The location of the spermine molecule in the major groove was unexpected as previous modeling studies (Liquori et al., 1967; Suwalsky et al., 1969) had predicted that polyamines such as spermine and spermidine were likely to bind in the minor groove.

Competitive binding experiments involving actinomycin D and ethidium bromide provide evidence in support of the intercalation model. These experiments indicate that both actinomycin D and ethidium bromide displace AFB1 from its binding sites on $d(ATGCAT)_2$. In contrast, binding of spermidine does not displace AFB1 from its binding sites on $d(ATGCAT)_2$. The latter experiment is somewhat more difficult to interpret, since the binding site for spermidine on $d(ATGCAT)_2$ is not known. The conformation of spermidine and the crystal structure with spermine for $d(CGCGAATTCGCG)_2$ (Drew & Dickerson, 1981) suggest that the spermidine is a groove binder, although its location is uncertain. It was observed that in the presence of spermidine and $d(ATGCAT)_2$ the chemical shifts of the AFB1 protons were shifted slightly upfield as compared to a sample that contained an equivalent amount of $d(ATGCAT)_2$ and AFB1 in the absence of spermidine. This suggests that AFB1 association is favored in the presence of spermidine, possibly as a result of greater thermal stabilization of the oligodeoxynucleotide.

We can rule out the possibility that AFB1 binding occurs predominantly at the ends of the oligodeoxynucleotide, on the basis of the competitive binding experiments. The addition of actinomycin D should not have affected potential AFB1 binding sites at the ends of the oligodeoxynucleotide. In fact, since the binding of actinomycin D increases the thermal stability of the oligodeoxynucleotide duplex, one might expect to see increased binding of the carcinogen to the oligodeoxynucleotide in the presence of the actinomycin D, were the carcinogen binding to the ends of the oligomer. Likewise, if end stacking were the primary phenomenon occurring for AFB1, then the AFB1 chemical shifts would be unaffected by low levels of ethidium bromide. Figure 7 shows that this is not the case. The AFB1 proton chemical shift changes decrease in a gradual and continuous manner as the concentration of ethidium bromide is increased.

Displacement of AFB1 by actinomycin D or ethidium bromide does not provide unequivocal evidence that the actinomycin D or ethidium molecules are binding at the same site as AFB1. An alternative scenario which could explain this result is that the binding of actinomycin D or ethidium bromide alters the oligodeoxynucleotide conformation such that the binding site for AFB1 is disrupted. The competitive binding experiments provide evidence consistent with intercalation as a model for the AFB1–$d(ATGCAT)_2$ interaction. Misra et al. (1983) examined the effect of ethidium bromide on the *covalent* binding of AFB1 to pBR322 DNA. Their experiments showed that, in the presence of ethidium bromide, the covalent reaction of AFB1 to the DNA was substantially reduced. Their observations, and our results which show that the presence of ethidium bromide inhibits the equilibrium binding of AFB1, support the hypothesis that the precovalent orientation of the carcinogen involves intercalation.

To obtain additional evidence in support of an intercalation model for the interaction of AFB1 with DNA, equilibrium binding of the carcinogen to supercoiled plasmid pBR322 was examined. The ability of AFB1 to unwind and rewind the supercoiled plasmid provides corroborating evidence for the intercalation model (Waring, 1970; Espejo & Lebowitz, 1976). Unwinding results in the removal of supercoils from the closed circular plasmid DNA and is readily quantitated by techniques sensitive to the tertiary structure of the DNA molecule, such as gel electrophoresis. Nonintercalative binding can also affect electrophoretic mobility of DNA, if the binding involves charge neutralization or a change in the persistence length of the DNA molecule. The latter was observed in the case of covalent *cis*-dichlorodiammineplatinum(II)–DNA adducts (Cohen et al., 1979; Ushay et al., 1981). With noncovalently bound molecules, however, nonintercalative binding would not be expected to introduce positive supercoils into relaxed closed circular DNA (Figure 9B). Furthermore, AFB1 is a neutral species and association of the carcinogen with the plasmid should not affect the negative charge on the DNA.

Orientation of Bound AFB1 Molecules. Chemical shift data, competitive binding experiments, and the gel electrophoresis data with pBR322 are consistent with intercalative binding. The oligodeoxynucleotide contains five potential sites where the AFB1 molecule could intercalate (or partially intercalate) with more than one geometry. Unfortunately, ^1H NOE experiments designed to reveal specific dipolar interactions between the AFB1 molecule and $d(ATGCAT)_2$ were inconclusive, presumably because of the low solubility of AFB1. However, the results of T_1 and T_2 relaxation studies described here suggest binding involves the dA·dT base pairs on the oligodeoxynucleotide. This is consistent with evidence derived from studies on polymeric DNA (Stone et al., 1988) which suggests that the AFB1 molecule can interact with dA·dT as well as dG·dC base pairs. Presumably, only dG·dC interactions lead to subsequent covalent attachment of the carcinogen. In the oligodeoxynucleotide system, it is likely

that transient intercalation of AFB1 is occurring at multiple potential intercalation sites, with comparable binding constants.

Covalent attachment occurs at the guanine N7 position with high stereoselectivity. Examination of molecular models indicates that the AFB1 molecule can be intercalated into the B-DNA helix in an orientation such that the *exo*-8,9-epoxide species is correctly oriented for attack at N7 of guanine. This orientation of AFB1 would position the carcinogen on the 5′ face of guanine with the AFB1 H5 proton above the purine ring and thus would be expected to result in a substantial ring-current shielding for the H5 proton, consistent with our experimental results (Table II). An intercalation model for covalently bound AFB1 has recently been considered in a molecular modeling study by E. L. Loechler and co-workers (Loechler et al., 1988). Intercalation was compared with major groove binding for the AFB1–N7 guanine adduct, and it was concluded that the latter orientation for the bound carcinogen was favored. One major groove binding orientation could explain previously obtained sequence-specific binding data (Benasutti et al., 1988), although Loechler et al. (1988) cautioned that their calculations ignore potentially significant contributions of entropic/solvation terms in the interaction of AFB1 with DNA. AFB1 might interact with DNA both via intercalation and, for specific high-affinity sequences, from the major groove. While a major groove location for covalently bound AFB1 could exist, the present results support intercalative noncovalent association between AFB1 and B-DNA. We emphasize that verification of the conformation of AFB1–DNA adducts must await experimental evidence from analysis of adducts with several sequences. Such experiments are currently in progress in this laboratory.

Acknowledgments

We thank Drs. Elliot Gruskin and Stephen Lloyd for helpful advice with gel electrophoresis experiments, which utilized the Molecular Genetics Core Facilities in the Molecular Toxicology Center.

Registry No. AFB1, 1162-65-8; d(ATGCAT), 53263-13-1.

References

Benasutti, M., Ejadi, S., Whitlow, M. D., & Loechler, E. L. (1988) *Biochemistry 27*, 472–481.

Black, H. S., & Jirgensons, B. (1967) *Plant Physiol. 42*, 731–735.

Bodenhausen, G., Kogler, H., & Ernst, R. R. (1984) *J. Magn. Reson. 58*, 370–388.

Chiao, Y.-C. C., & Krugh, T. R. (1977) *Biochemistry 16*, 747–755.

Clifford, J. I., & Rees, K. R. (1967) *Biochem. J. 108*, 467–471.

Cohen, G. L., Bauer, W. R., Barton, J. K., & Lippard, S. J. (1979) *Science (Washington, D.C.) 203*, 1014–1016.

Drew, H. R., & Dickerson, R. E. (1981) *J. Mol. Biol. 151*, 535–556.

Espejo, R. T., & Lebowitz, J. (1976) *Anal. Biochem. 72*, 95–103.

Essigmann, J. M., Croy, R. G., Nadzan, A. M., Busby, W. F., Jr., Reinhold, V. N., Büchi, G., & Wogan, G. N. (1977) *Proc. Natl. Acad. Sci. U.S.A. 74*, 1870–1874.

Essigmann, J. M., Green, C. L., Croy, R. G., Fowler, K. W., Büchi, G. H., & Wogan, G. N. (1983) *Cold Spring Harbor Symp. Quant. Biol. 47*, 327–337.

Fujimoto, S., & Ohba, Y. (1975) *J. Biochem. 77*, 187–195.

Giessner-Prettre, C., & Pullman, B. (1976) *Biochem. Biophys. Res. Commun. 70*, 578–581.

Giessner-Prettre, C., & Pullman, B. (1982) *Biochem. Biophys. Res. Commun. 107*, 1539–1544.

Giessner-Prettre, C., Pullman, B., Borer, P. N., Kan, L.-S., & Ts'o, P. O. P. (1976) *Biopolymers 15*, 2277–2286.

Giessner-Prettre, C., Ribas Prado, F., Pullman, B., Kan, L.-S., Kast, J. R., & Ts'o, P. O. P. (1981) *Comput. Programs Biomed. 13*, 167–183.

Israel-Kalinsky, H., Tuch, J., Roitelaman, J., & Stark, A. A. (1982) *Carcinogenesis (London) 3*, 423–429.

Kanne, D., Straub, K., Hearst, J. E., & Rapoport, H. (1982) *J. Am. Chem. Soc. 104*, 6754–6764.

King, A. M. Q., & Nicholson, B. H. (1969) *Biochem. J. 114*, 679–687.

Krugh, T. R., & Neely, J. W. (1973) *Biochemistry 12*, 4418–4425.

Krugh, T. R., & Chen, Y. C. (1975) *Biochemistry 14*, 4912–4922.

Krugh, T. R., & Reinhardt, C. G. (1975) *J. Mol. Biol. 97*, 133–162.

LePecq, J.-B. (1971) in *Methods Biochem. Anal. 20*, 41–86.

Liquori, A. M., Costantino, L., Crescenzi, V., Elia, V., Giglio, E., Puliti, R., De Santis Savino, M., & Vitagliano, V. (1967) *J. Mol. Biol. 24*, 113–122.

Loechler, E. L., Teeter, M. M., & Whitlow, M. D. (1988) *J. Biomol. Struct. Dyn. 5*, 1237–1257.

Marien, K., Moyer, R., Loveland, P., Van Holde, K., & Bailey, G. (1987) *J. Biol. Chem. 262*, 7455–7462.

Misra, R. P., Muench, K. F., & Humayun, M. Z. (1983) *Biochemistry 22*, 3351–3359.

Muench, K. F., Misra, R. P., & Humayun, M. Z. (1983) *Proc. Natl. Acad. Sci. U.S.A. 80*, 6–10.

Neely, W. C., Lansden, J. A., & McDuffie, J. R. (1970) *Biochemistry 9*, 1862–1866.

Patel, D. J. (1974) *Biochemistry 13*, 2396–2402.

Reinhardt, C. G., & Krugh, T. R. (1978) *Biochemistry 17*, 4845–4854.

Rosenberg, L. S., Balakrishnan, M. S., Graves, D. E., Lee, K. R., Winkle, S. A., & Krugh, T. R. (1982) in *Biological Activities of Polymers* (Carraher, C. E., & Gebelein, C. G., Eds.) ACS Symposium Series 186, pp 269–281, American Chemical Society, Washington, DC.

Sobell, H. M., & Jain, S. C. (1972) *J. Mol. Biol. 68*, 21–34.

Sporn, M. B., Dingman, C. W., Phelps, H. L., & Wogan, G. N. (1966) *Science (Washington, D.C.) 151*, 1539–1541.

Stone, M. P., Gopalakrishnan, S., Harris, T. M., & Graves, D. E. (1988) *J. Biomol. Struct. Dyn. 5*, 1025–1041.

Straub, K., Kanne, D., Hearst, J. E., & Rapoport, H. (1981) *J. Am. Chem. Soc. 103*, 2347–2355.

Suwalsky, M., Traub, W., Shmueli, U., & Subriana, J. A. (1969) *J. Mol. Biol. 42*, 363–373.

Takusagawa, F., Dabrow, M., Neidle, S., & Berman, H. M. (1982) *Nature (London) 296*, 466–469.

Ushay, H. M., Tullius, T. D., & Lippard, S. J. (1981) *Biochemistry 20*, 3744–3748.

Waring, M. J. (1970) *J. Mol. Biol. 54*, 247–279.

Winkle, S. A., Rosenberg, L. S., & Krugh, T. R. (1982) *Nucleic Acids Res. 10*, 8211–8223.

Woo, N. H., Seeman, N. C., & Rich, A. (1979) *Biopolymers 18*, 539–552.

Wüthrich, K. (1986) *NMR of Proteins and Nucleic Acids*, Wiley, New York.